

Cite this: DOI: 10.1039/c0jm04567e

www.rsc.org/materials

PAPER

## Incorporating triphenyl sulfonium salts in polyfluorene PLEDs: an all-organic approach to improved charge injection

Dimitra G. Georgiadou,<sup>ac</sup> Leonidas C. Palilis,<sup>ad</sup> Maria Vasilopoulou,<sup>a</sup> George Pistolis,<sup>b</sup> Dimitra Dimotikali<sup>c</sup> and Panagiotis Argitis<sup>\*a</sup>

Received 29th December 2010, Accepted 26th April 2011

DOI: 10.1039/c0jm04567e

All-organic sulfonium salts are introduced as a class of ionic compounds that show high compatibility with conjugated polymers and may form blends with attractive luminescent properties leading to significant improvement in single-layer polymer light emitting diodes' (PLEDs') performance. We demonstrate that triphenylsulfonium (TPS) triflate:polyfluorene-co-benzothiadiazole (F8BT)-blend based PLEDs show a lower turn-on voltage, an increased luminous efficiency and higher peak luminance values. These results are being rationalized in terms of anionic accumulation and space charge formation at the anode side, which facilitates hole injection, leading to more balanced injection and subsequently to a higher recombination rate. Moreover, we find that the salt anion size plays a critical role in the device operating characteristics. The judicious choice of both the salt and the emitting polymer by considering relative energy level alignment, salt electrochemical stability and acquired thermodynamic stability of blend morphology is important for the achievement of high performance PLEDs without requiring elaborate device architectures.

### 1 Introduction

Organic Light Emitting Diodes (OLEDs)<sup>1</sup> have already entered successfully the display market,<sup>2</sup> whereas in the last decade a tremendous progress has been made in white light applications (WOLEDs), whose efficiencies have surpassed those of incandescent light sources.<sup>3,4</sup> Furthermore, technological approaches that can lead to device performance improvement, while using low cost and easy to implement methods in industrial level processes and simplified device architectures, are under intense investigation. In this context, OLEDs based on conjugated polymers (termed as PLEDs)<sup>5</sup> seem to become more attractive for lighting and large area applications due to their easier processability by solution deposition techniques. In addition, to further simplify the device architecture and reduce the production cost, air stable cathodes (Al, Ag *etc.*) are required. However, issues related to the fact that such metallic cathodes usually have a high work function, translated to a large injection barrier towards the polymer Lowest Unoccupied Molecular Orbital (LUMO), must be addressed.

The incorporation of mobile ions in the active layer of polymer light emitting devices has been proposed as a means of improving charge injection and transport and is a frequently adopted strategy for improving device performance.<sup>6</sup> The most prominent example is the Polymer Light Emitting Electrochemical Cell (PLEC), where, according to the electrochemical doping model,<sup>7</sup> a p-n junction is formed *in situ* in the active layer upon application of a bias due to the p- and n- doping of the polymer at the anode and cathode respectively, or alternatively, according to the electrodynamic model, upon application of a small bias and for high ionic density, the ions drift to the electrodes and the local electric field is maximized there, facilitating charge injection.<sup>8</sup> As a result, a balanced electron and hole injection and consequently high current density and electroluminescence quantum efficiency at low voltage can be obtained.

A major drawback of devices incorporating ions is the slow device turn-on and the need for a pre-biasing before operation, due to the generally slow ion motion. This problem was addressed by introducing in the standard ternary PLEC system the concept of frozen junctions<sup>9</sup> and by using novel electrolytes.<sup>10</sup> Moreover, ionic liquids seem to be quite advantageous, since they can be readily mixed with a conjugated polymer and form a binary stable system that shows no macroscopic phase separation, has good ionic conductivity and improves device efficiency.<sup>11,12</sup> Finally, several groups have proposed doping of conjugated polymers with inorganic (*i.e.* FeCl<sub>3</sub>,<sup>13</sup> LiBr<sup>14</sup>) or organic salts (*i.e.* the well-known supporting electrolytes Bu<sub>4</sub>NPF<sub>6</sub>,<sup>15</sup> Bu<sub>4</sub>NBF<sub>4</sub>,<sup>16</sup> TEAP,<sup>17</sup> *etc.*), requiring though usually

<sup>a</sup>Institute of Microelectronics, National Centre for Scientific Research "Demokritos", PO Box 60228, 15310 Athens, Greece. E-mail: argitis@imel.demokritos.gr

<sup>b</sup>Institute of Physical Chemistry, National Centre for Scientific Research "Demokritos", 15310 Athens, Greece

<sup>c</sup>Department of Chemical Engineering, National Technical University of Athens, 15780 Athens, Greece

<sup>d</sup>Department of Physics, University of Patras, 26500 Patras, Greece

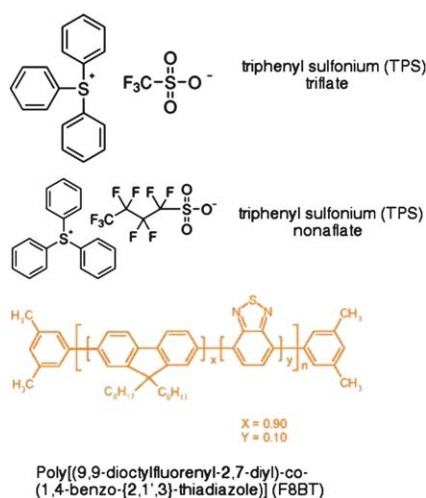


Fig. 1 Molecular structure of TPS-salts and F8BT copolymer.

a thermal and/or electrical treatment step for the activation of the salt.<sup>18,19</sup>

In this paper, we propose the use of organic sulfonium salts as a new class of ionic compounds with attractive characteristics that can improve charge injection in polymer light emitting devices. Sulfonium salts are a well known class of photoacid generators (PAGs) applied in lithographic imaging processes, catalyzing deprotection or crosslinking reactions of certain photoresists.<sup>20–22</sup> Recently, triphenylsulfonium (TPS) triflate was used by our group inside a poly(9-vinylcarbazole) (PVK) matrix along with two emitters in order to achieve photochemical (under UV illumination) tuning of the emission colour by protonation of emitter basic sites and definition of the three subpixels (RGB) in a single-layer PLED.<sup>23,24</sup> Here, we use a triphenyl sulfonium (TPS) salt having mobile triflate anions that can be readily mixed at high concentrations with a polyfluorene-based conjugated copolymer in solution and then processed as an effective active layer in single-layer PLEDs leading to considerably improved performance without demanding any thermal or electrical pretreatment. The sulfonium salt addition in the emissive layer improves charge, in particular hole, injection as a result of anionic movement, accumulation and space charge formation at the anode–polymer interface, leading to lower turn-on and operating voltage as well as higher current luminous and power efficiencies.

## 2 Experimental section

The polyfluorene copolymer poly[(9,9-dioctylfluorenyl-2,7-diyl)-co-(1,4-benzo-{2,1',3}-thiadiazole)] (F8BT) was purchased from American Dye Source Inc. Poly(3,4-ethylenedioxythiophene):poly(styrenesulfonate) (PEDOT:PSS) was provided by Aldrich. The sulfonium salts used in this work, having the same cation, triphenylsulfonium (TPS), and two different anions, trifluoromethane sulfonate (triflate) and perfluoro-1-butanefluorobutanesulfonate (nonaflate), were purchased from Midori Kagaku Co., Ltd.

Single-layer polymer light emitting diodes (PLEDs) were fabricated on oxygen plasma pre-cleaned transparent glass substrates coated with indium tin oxide (ITO). A 60 nm thick

PEDOT:PSS film was spin-coated from a pre-filtered (through a 0.45  $\mu\text{m}$  PVDF filter) aqueous solution onto ITO and annealed in air at 135  $^{\circ}\text{C}$  for at least 15 min. The emitting layer was spin-cast from an 8 mg ml<sup>-1</sup> F8BT chloroform solution (pre-filtered through a 0.20  $\mu\text{m}$  PTFE filter) containing the sulfonium salt in different concentrations (% w/w per polymer mass) resulting in a film thickness of about 90 nm. All polymer films were annealed at 80  $^{\circ}\text{C}$  for 10 min in air. Finally, a  $\sim$ 200 nm thick Al cathode was deposited by thermal evaporation through a shadow mask (defined active area of 12.56 mm<sup>2</sup>) to complete the device structure. Current–voltage characteristics of the fabricated PLEDs were measured with a Keithley 2400 source–measure unit and luminance and electroluminescence spectral characteristics were recorded with an Ocean Optics spectrophotometer equipped with fiber optics, assuming a Lambertian emission profile (for the luminance measurements). All organic layers' deposition was carried out in ambient conditions and all device measurements were conducted immediately after their fabrication in air without any encapsulation.

Film photoluminescence spectra were recorded with a Perkin-Elmer LS-50B fluorescence spectrometer and time-resolved fluorescence measurements were determined using the time-correlated single-photon counter FL900 of Edinburgh Instruments.

The surface structure and morphology of the F8BT polymer film upon insertion of TPS-triflate was studied with an NT-MDT Atomic Force Microscope (AFM) operated in semicontact (tapping) mode.

## 3 Results and discussion

### 3.1 Optical and electronic properties of TPS-salt:F8BT blend

The molecular structures of the polyfluorene copolymer poly[(9,9-dioctylfluorenyl-2,7-diyl)-co-(1,4-benzo-{2,1',3}-thiadiazole)] (F8BT) and triphenyl sulfonium (TPS)-salts used in this work are presented in Fig. 1. F8BT is an excellent bipolar conjugated copolymer with similar electron and hole mobilities ( $\sim 10^{-3}$  cm<sup>2</sup> V<sup>-1</sup> s<sup>-1</sup>)<sup>25</sup> and high (>70%) photoluminescence (PL) quantum yield.<sup>26</sup> Recently, high performance PLEDs based on F8BT have been reported by Friend *et al.* following different

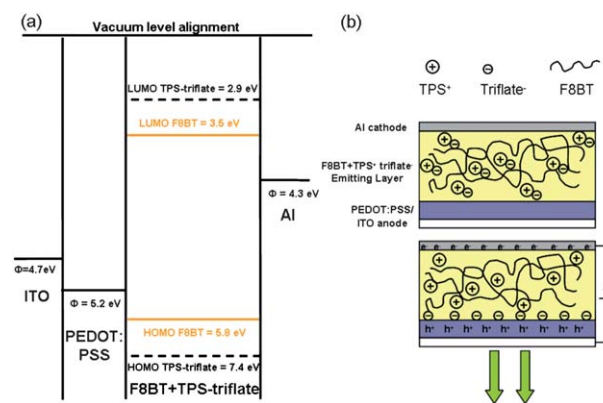
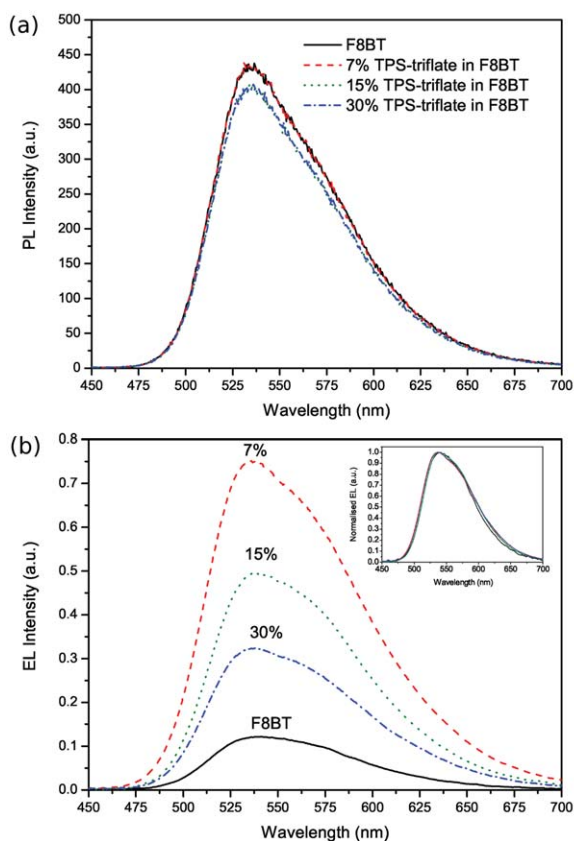


Fig. 2 (a) Energy level diagram of PLEDs assuming vacuum level alignment. (b) Simplified schematic PLED structure depicting the ions' placement before and after the application of a positive bias.



**Fig. 3** (a) PL and (b) EL spectra of pristine F8BT film (solid line) and films with 7% (dashed line), 15% (dotted line) and 30% (dash-dot line) TPS-triflate added in F8BT. The PL films were all excited at 375 nm and the spectra were taken under identical conditions, so that their intensities can be compared. The EL spectra were all recorded at 15 V. (Inset) Normalised EL spectra.

optimization approaches.<sup>27,28</sup> Moreover, it was chosen because it has a relatively low lying LUMO at 3.5 eV below vacuum,<sup>29</sup> lower than that of TPS-triflate ( $\sim 3$  eV) as calculated from cyclic voltammetry.<sup>30,31</sup> Fig. 2a depicts the tentative energy diagram of the F8BT:TPS triflate-based PLED structure in a flat-band configuration (assuming vacuum level alignment occurs at the various interfaces). This energy level configuration, combined with the very large optical band gap of TPS-triflate (4.4 eV as calculated from the onset of the UV-Vis absorption spectrum<sup>22</sup>), has the direct consequence that no energy or electron transfer is expected to occur from F8BT to TPS-triflate molecules in contrast to previously reported results,<sup>32</sup> allowing efficient exciton formation and recombination to take place inside the F8BT.

Indeed, as it can be seen in Fig. 3a, the PL spectra of F8BT are not influenced by the TPS-triflate addition and, even at high (30%) salt concentrations, PL intensity shows only marginal decrease of about 6% compared to pristine F8BT, probably due to salt aggregate formation (*vide infra*), that may affect F8BT PL decay in the vicinity of these aggregates. Furthermore, time-resolved PL spectroscopy showed that the primary F8BT exciton lifetime does not change upon addition of the TPS-triflate (2.5 ns for F8BT film and 2.8 ns for films containing the TPS-triflate at various concentrations—lifetimes measured at 380 nm and

530 nm excitation and emission wavelength respectively), indicating that no detrimental interaction takes place between ions and excitons, as reported *ie.* for conjugated polyelectrolytes bearing ionic side chains mixed with F8BT.<sup>33</sup>

Finally, it should be emphasized that the wide electrochemical stability window of TPS-triflate encompasses both the n- and p-doping potentials of F8BT (as derived by their HOMO and LUMO levels), rendering the (irreversible) reduction of the TPS-triflate—which could lead to shortening of the device operational lifetime and negatively affect device stability (ref. 34 and 35)—thermodynamically unlikely and thus, represents a very advantageous characteristic of this blend.

### 3.2 PLED device performance

As a next step, PLEDs based on varying F8BT:TPS-triflate blend compositions having the simple sandwich structure depicted in Fig. 2b were fabricated and characterised. The current density–voltage ( $J$ – $V$ ) and luminance–voltage ( $L$ – $V$ ) characteristics of those devices (Fig. 4) reveal a significantly improved performance, even for the device with the lowest TPS-triflate concentration (7% w/w), compared to reference devices. For instance, for the device with 7% TPS-triflate at 16 V the current density is doubled ( $2787 \text{ A m}^{-2}$  compared to  $1310 \text{ A m}^{-2}$  for the F8BT-based PLED) and we observe an almost 12-fold increase of the luminance ( $3253 \text{ cd m}^{-2}$  versus  $277 \text{ cd m}^{-2}$  for the reference device). In general, in the PLEDs based on TPS-triflate:F8BT blends current and especially luminance increase more abruptly

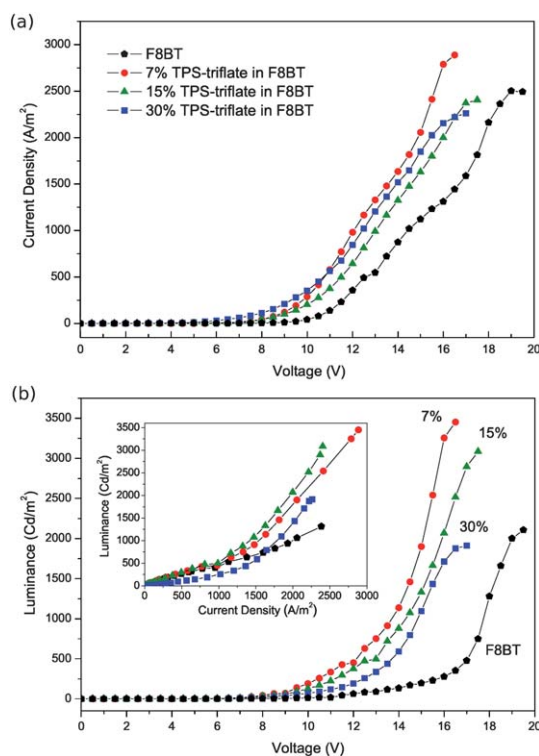


**Fig. 4** (a) Current density–voltage, (b) luminance–voltage and (inset) luminance–current density characteristics of F8BT-based PLEDs with 0% (pentagons—reference devices), 7% (circles), 15% (triangles) and 30% (squares) TPS-triflate.

than in F8BT-based devices. Furthermore, a decrease of the turn-on voltage (here defined as the voltage where  $L = 1 \text{ cd m}^{-2}$ ) from 7.5 V for the reference PLED to 4.5 V for the devices with the TPS-salt was observed (see also Table 1). This improvement was attributed to an increase of the hole injection rate at the polymer–anode interface, likely as a result of the lowering of the injection barrier at this interface. Hence, it is suggested that upon application of an external bias the triflate anions drift to the anode and accumulate there forming a space charge (which is equivalent to p-type doping of F8BT close to the anode interface). Note that charge neutrality at the interface may be preserved by compensation of salt anions from the injected holes. The TPS cations, which may be similarly expected to drift towards the cathode, are considered to move much slower due to their bulky size or even remain in their initial position (see schematic representation in Fig. 2b) and thus, no discrete p–n junction may be readily formed. If this were the case, then: (1) both contact electrodes should become ohmic, resulting in a turn-on voltage comparable to the optical band gap of F8BT (about 2.3 V), (2) the device should emit light in both forward and reverse bias, indeed symmetrically, (3) a delayed device turn-on and (4) a difference between first and second scans should also be observed. Nevertheless, none of the above was noticed in our devices and thus, we attribute this improved performance to the fast anions' movement and their subsequent accumulation at the anode side resulting in a lowering of the effective work function for hole injection.

To further support this argument, we compare in Fig. 5 the  $J$ – $V$ – $L$  characteristics of F8BT-based PLEDs doped with 7% TPS-triflate and 7% TPS-nonaflate. The molecular structure of TPS-nonaflate is shown in Fig. 1 and it is obvious that the size of nonaflate anion is larger than triflate. Both the current density and luminance increase faster for the device with the smaller anion size (triflate) and therefore are supportive of our hypothesis that the anion size does play a critical role in the device performance. Experiments with different anion sizes and the same cation (TPS) in a wide band gap polyfluorene matrix are also currently underway by our group providing data in agreement with this hypothesis and will be presented in detail in a forthcoming publication.<sup>36</sup> Note that our devices were not subsequent to any type of “activation” in terms of thermal or electrical treatment, which would increase ionic conductivity as reported by other groups working with similar salts.<sup>18,19</sup>

If we examine in more detail the TPS-triflate concentration dependence on PLED characteristics as presented in Fig. 4, we notice that the current density–voltage characteristics and the turn-on voltage do not seem to be significantly dependent on the TPS-triflate concentration. This indicates that charge transport is conducted almost entirely through the F8BT phase.

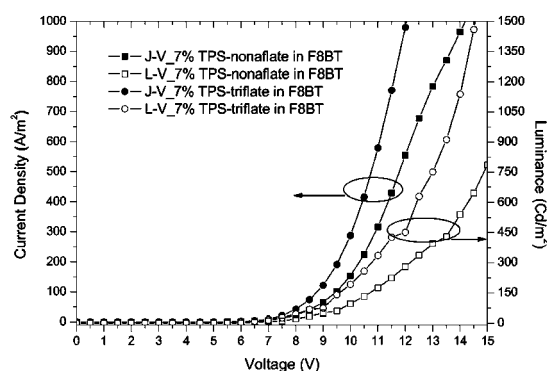


**Fig. 5** Current density–voltage (closed symbols) and luminance–voltage (open symbols) characteristics of F8BT-based PLEDs with 7% TPS-triflate (circles) and 7% TPS-nonaflate (squares) added in the emitting layer.

TPS-triflate molecules may only assist in improving hole injection and then transfer to F8BT, as expected by the relative placement of the F8BT polymer and the TPS-triflate energy levels (see Fig. 2a). However, as the concentration of the TPS-triflate increases, the device luminance tends to decrease, whereas the current density remains relatively stable, and as a consequence the efficiencies decrease too (see inset in Fig. 3, where the slope of the  $L$ – $J$  plot represents the current luminous efficiency of each device). More specifically, the luminous current and power efficiencies at 16 V increase from  $0.2 \text{ cd A}^{-1}$  and  $0.04 \text{ lm W}^{-1}$  for the reference device to  $1.16 \text{ cd A}^{-1}$  and  $0.23 \text{ lm W}^{-1}$  for the device with 7% w/w TPS-triflate, respectively. These values slightly decrease as TPS-triflate concentration is increased but they remain still higher than those of the reference device ( $1.03 \text{ cd A}^{-1}$  and  $0.21 \text{ lm W}^{-1}$  for 15% and  $0.84 \text{ cd A}^{-1}$  and  $0.16 \text{ lm W}^{-1}$  for 30% w/w TPS-triflate, respectively). A similar trend holds for the maximum values of those devices as depicted in Table 1. The electroluminescence spectra of PLEDs with different TPS-triflate concentrations at 15 V are shown in Fig. 3b. The normalised spectra (inset) clearly indicate that the electroluminescence is not influenced by the added salt, namely the emissive state is attributed exclusively to F8BT (compare also EL with PL spectra). The luminance decrease and the consequent reduction of the device efficiency as the TPS-triflate concentration increases may be attributed to increased non-radiative recombination in the vicinity of salt molecules (as also suggested from the PL measurements) or to increased ion–exciton interactions that facilitate exciton quenching.<sup>37</sup> Here, we should also mention that the performance of the device could be further improved with the implementation of a low work function cathode (*i.e.* Ca, Ba, LiF/Al) or a suitable electron

**Table 1** Device characteristics of F8BT-based PLEDs with different TPS-triflate concentrations

TPS-triflate concentration (w/w)	$V_{\text{turn-on}}$ (V)	$J_{\text{max}}$ ( $\text{A m}^{-2}$ ) [at $V$ ]	$L_{\text{max}}$ ( $\text{cd m}^{-2}$ ) [at $V$ ]	Max luminous efficiency ( $\text{cd A}^{-1}$ ) [at $L$ ]	Max power efficiency ( $\text{lm W}^{-1}$ ) [at $L$ ]
0%	7.5	2500 [19 V]	2107 [19.5 V]	0.84 [2107 $\text{cd m}^{-2}$ ]	0.13 [2107 $\text{cd m}^{-2}$ ]
7%	4.5	2886 [16.5 V]	3451 [16.5 V]	1.19 [3451 $\text{cd m}^{-2}$ ]	0.23 [3253 $\text{cd m}^{-2}$ ]
15%	5	2403 [17.5 V]	3084 [17.5 V]	1.31 [2911 $\text{cd m}^{-2}$ ]	0.24 [3084 $\text{cd m}^{-2}$ ]
30%	5	2260 [17 V]	1912 [17 V]	0.88 [1794 $\text{cd m}^{-2}$ ]	0.16 [1876 $\text{cd m}^{-2}$ ]

injection layer at the polymer/Al interface. High performance F8BT-based Hy-LEDs due to efficient electron injection *via* a thin reduced transition metal oxide film<sup>38,39</sup> or a solution-processable polyoxometalate nanolayer<sup>40</sup> are already demonstrated by our group and they could be combined with the F8BT–sulfonium salt blends presented here to further enhance the device efficiencies.

### 3.3 Film morphology study

In order to investigate the effect of film morphology on device operation, in Fig. 6 we present Atomic Force Microscopy (AFM) topographic images of F8BT films containing different amounts of TPS-triflate. The pristine F8BT film (Fig. 6a) is very smooth with a very low surface roughness (RMS = 0.6 nm). Upon addition of 15% TPS-triflate to F8BT (Fig. 6b), the film becomes less smooth and rougher (RMS = 2 nm) but still shows no macroscopic phase separation, while allowing the formation of an interpenetrating network of F8BT–TPS molecules, which favours both ionic and electronic transport. If we double the TPS-triflate concentration to 30% (Fig. 6c), phase separation becomes clearly evident as TPS aggregates are being formed and the RMS roughness is further raised to 4.1 nm. Finally, when TPS-triflate reaches 50% (Fig. 6d), the aggregates grow bigger with an RMS roughness of almost 18 nm whereas the peak-to-valley height reaches 180 nm (a value much larger than the nominal film thickness). At such large concentrations, the preferred clustering and aggregation of the TPS-triflate molecules may provide a pathway for direct charge transport without recombination in the F8BT phase or even facilitate non-radiative exciton decay near them. Indeed, the smaller current luminous efficiency compared to the very high current density for PLEDs having 50% w/w TPS-triflate supports the proposed device operation mechanism.

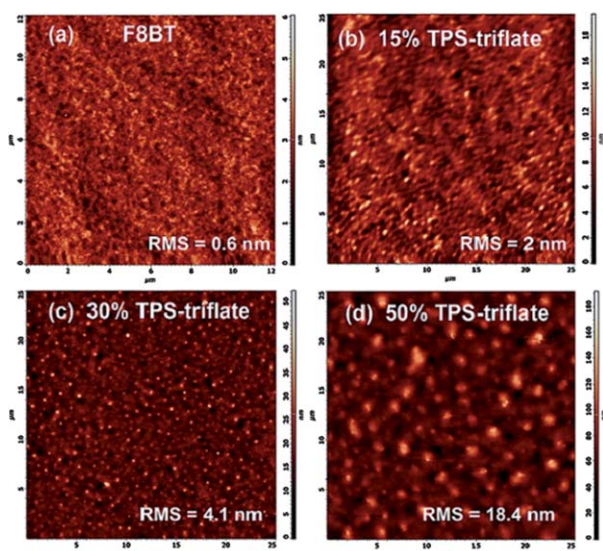


**Fig. 6** Semiconducting (tapping) mode AFM micrographs depicting the surface topography of 90 nm thick films of (a) pristine F8BT, (b) 15%, (c) 30% and (d) 50% TPS-triflate in F8BT spin-coated on quartz substrate. The root mean square (RMS) surface roughness is indicated in each case.

## 4 Summary

We demonstrate an improved performance of single-layer polyfluorene (F8BT)-based PLEDs by adding appropriate amounts of triphenylsulfonium (TPS) salts in the emitting layer. The addition of TPS-triflate in F8BT leads (up to a certain concentration) to improved device characteristics, which is attributed to enhanced hole injection as a result of the TPS anions' movement towards the anode, where they accumulate and create a space charge. This leads to a decrease of the device turn-on and operating voltage. It also improves charge balance and facilitates more efficient recombination inside the polymer matrix, as evidenced by the increased device efficiency. At an optimum TPS-triflate concentration, the luminous efficiency is maximized, whereas, at higher salt concentrations, TPS-triflate aggregate formation may provide a path to facilitate charge transport but also results in decreased recombination rates. On the other hand the presented results with TPS-nonaflate highlight the crucial role played by the anion size. All the devices investigated show no delay in response time and neither require an electrical or thermal pretreatment, in contrast to the commonly used PLECs.

These results clearly indicate that sulfonium salts, especially the all-organic ones that provide miscibility advantages and do not contain heavy atoms, are a very attractive class of ionic compounds that can be incorporated in single-layer PLEDs with high performance. Additionally, the possibility to independently vary their cation or anion provides ways for tuning both their energy levels and ion transport properties, and thus can provide a deeper understanding of the charge injection/transport mechanisms in organic light emitting devices. Finally, the addition of fluorinated compounds (such as triflate and nonaflate anions used here) inside PEDOT:PSS could offer an attractive alternative option for improvement of hole injection<sup>41</sup> and is currently under investigation by our group.

## Notes and references

- 1 C. W. Tang and S. A. Van Slyke, *Appl. Phys. Lett.*, 1987, **51**, 913.
- 2 O.-K. Song and H. Chung, *Inf. Disp.*, 2010, **10**, 14.
- 3 Y. Sun, N. C. Giebink, H. Kanno, B. Ma, M. E. Thompson and S. R. Forrest, *Nature*, 2006, **440**, 908.
- 4 A. Köhnen, M. Irion, N. Rehm, P. Yacharias and K. Meerholz, *J. Mater. Chem.*, 2010, **20**, 3301.
- 5 J. H. Burroughes, D. D. C. Bradley, A. R. Brown, R. N. Marks, K. Mackay, R. H. Friend, P. L. Burns and A. B. Holmes, *Nature*, 1990, **347**, 539.
- 6 Q. Pei, G. Yu, C. Zhang, Y. Yang and A. J. Heeger, *Science*, 1995, **269**, 1086.
- 7 Q. Pei, Y. Yang, G. Yu, C. Zhang and A. J. Heeger, *J. Am. Chem. Soc.*, 1996, **118**, 3922.
- 8 J. C. deMello, N. Tessler, S. C. Graham and R. H. Friend, *Phys. Rev. B: Condens. Matter*, 1998, **57**, 12951.
- 9 J. Gao, G. Yu and A. J. Heeger, *Appl. Phys. Lett.*, 1997, **71**, 1293.
- 10 S. Tang and L. Edman, *J. Phys. Chem. Lett.*, 2010, **1**, 2727.
- 11 S. Panozzo, M. Armand and O. Stephan, *Appl. Phys. Lett.*, 2002, **80**, 679.
- 12 R. Marcilla, D. Mecerreyes, G. Winroth, S. Brovelli, M. Del Mar Rodriguez Yebra and F. Cacialli, *Appl. Phys. Lett.*, 2010, **96**, 043308.
- 13 D. B. Romero, M. Schaer, L. Zuppiroli, B. Casar and B. Francois, *Appl. Phys. Lett.*, 1995, **67**, 1659.
- 14 W. Zhao and J. M. White, *Appl. Phys. Lett.*, 2005, **87**, 103503.
- 15 C. C. Yap, M. Yahaya and M. M. Salleh, *Curr. Appl. Phys.*, 2009, **9**, 722.
- 16 Y. Sakuratani, M. Asai, M. Tokita and S. Miyata, *Synth. Met.*, 2001, **123**, 207.

- 17 E. Itoh, T. Yamashita and K. Miyairi, *J. Appl. Phys.*, 2002, **92**, 5971.
- 18 S. S. Oh, J. H. Park, S. W. Kim and B. Park, *J. Appl. Phys.*, 2007, **102**, 074503.
- 19 Y. Shao, G. C. Bazan and A. J. Heeger, *Adv. Mater.*, 2007, **19**, 365.
- 20 J. V. Crivello, *Adv. Polym. Sci.*, 1984, **62**, 1.
- 21 J. V. Crivello and J. H. W. Lam, *J. Polym. Sci., Polym. Chem. Ed.*, 1978, **16**, 2441.
- 22 E. Reichmanis, F. M. Houlihan, O. Nalamasu and T. X. Neenan, *Chem. Mater.*, 1991, **3**, 394.
- 23 M. Vasilopoulou, D. Georgiadou, G. Pistolis and P. Argitis, *Adv. Funct. Mater.*, 2007, **17**, 3477.
- 24 D. G. Georgiadou, M. Vasilopoulou, G. Pistolis, L. C. Palilis, D. Dimotikali and P. Argitis, *Phys. Status Solidi A*, 2008, **205**, 2526.
- 25 Y. Kim, S. Cook, S. A. Choulis, J. Nelson, J. R. Durrant and D. D. C. Bradley, *Chem. Mater.*, 2004, **16**, 4812.
- 26 N. Corcoran, A. C. Arias, J. S. Kim, J. D. MacKenzie and R. H. Friend, *Appl. Phys. Lett.*, 2003, **82**, 299.
- 27 D. Kabra, L. P. Lu, M. H. Song, H. J. Snaith and R. H. Friend, *Adv. Mater.*, 2010, **22**, 3194.
- 28 K.-H. Yim, W. J. Doherty, W. R. Salaneck, C. E. Murphy, R. H. Friend and J.-S. Kim, *Nano Lett.*, 2010, **10**, 385.
- 29 A. J. Campbell, D. D. C. Bradley and H. Antoniadis, *Appl. Phys. Lett.*, 2001, **79**, 2133.
- 30 F. D. Saeva and B. P. Morgan, *J. Am. Chem. Soc.*, 1984, **106**, 4121.
- 31 F. D. Saeva, D. T. Breslin and P. A. Martic, *J. Am. Chem. Soc.*, 1989, **111**, 1328.
- 32 S. Fung, S. C. Moratti, S. C. Graham and R. H. Friend, *Synth. Met.*, 1999, **102**, 1167.
- 33 J. Hodgkiss, G. Tu, S. Albert-Seifried, W. T. S. Huck and R. H. Friend, *J. Am. Chem. Soc.*, 2009, **131**, 8913.
- 34 Y. Kervella, M. Armand and O. Stephan, *J. Electrochem. Soc.*, 2001, **148**, H155.
- 35 J. Fang, P. Matyba, N. D. Robinson and L. Edman, *J. Am. Chem. Soc.*, 2008, **130**, 4562.
- 36 D. G. Georgiadou, M. Vasilopoulou, L. C. Palilis, G. Pistolis, D. Dimotikali and P. Argitis, manuscript in preparation.
- 37 J. Fang, P. Matyba and L. Edman, *Adv. Funct. Mater.*, 2009, **19**, 2671.
- 38 M. Vasilopoulou, L. C. Palilis, D. G. Georgiadou, A. M. Douvas, P. Argitis, S. Kennou, L. Syggelou, G. Papadimitropoulos, I. Kostis, N. A. Stathopoulos and D. Davazoglou, *Adv. Funct. Mater.*, 2011, **21**, 1489.
- 39 M. Vasilopoulou, L. C. Palilis, D. G. Georgiadou, P. Argitis, S. Kennou, L. Syggelou, I. Kostis, G. Papadimitropoulos, N. Konofaos, A. A. Iliadis and D. Davazoglou, *Appl. Phys. Lett.*, 2011, **98**, 123301.
- 40 L. C. Palilis, M. Vasilopoulou, D. G. Georgiadou and P. Argitis, *Org. Electron.*, 2010, **11**, 887.
- 41 T.-W. Lee, Y. Chung, O. Kwon and J.-J. Park, *Adv. Funct. Mater.*, 2007, **17**, 390.